

## Polarized neutron studies of forbidden magnons in the two-dimensional ferromagnet $K_2CuF_4$

W-H. Li, C. H. Perry, and J. B. Sokoloff

*Department of Physics, Northeastern University, Boston, Massachusetts 02115*

V. Wagner

*Physikalisch-Technische Bundesanstalt, Braunschweig, Federal Republic of Germany*

M. E. Chen and G. Shirane

*Brookhaven National Laboratory, Upton, New York 11719*

(Received 14 April 1986)

Polarized inelastic neutron scattering has been used to study the spin dynamics of the quasi-two-dimensional nonmetallic Heisenberg ferromagnet  $K_2CuF_4$  in weak magnetic fields at temperature in the vicinity of  $T_C$ . We have observed underdamped allowed and "forbidden" excitations in constant- $Q$  scans for two different applied magnetic fields over the temperature range from  $0.9T_C$  to  $2.9T_C$ . A frequency difference between the allowed magnon and its forbidden counterpart (with the allowed magnon being slightly higher) was also observed. The difference between the allowed and forbidden magnon integrated intensities was found to be directly proportional to the overall magnetization for the two different fields applied. The observations are in agreement with the slowly fluctuating spin-density theory of itinerant ferromagnetism. Surprisingly, the reduction in magnon frequency with increasing temperature follows a  $T^{5/2}$  over a wide temperature range. Such dependence is much like that which occurs at low temperatures.

### I. INTRODUCTION

$K_2CuF_4$  is a colorless, optically transparent nonmetallic quasi-two-dimensional ferromagnetic crystal with  $T_C = 6.25$  K in zero field.<sup>1</sup> Hidaka and Walker<sup>2</sup> reported that a very small but finite orthorhombic lattice distortion destroys the square planar arrangement of the  $Cu^{2+}$  ions in  $K_2CuF_4$ . This leads to a doubling of the  $D_{4h}^5$  crystallographic unit cell, probably resulting in the space group  $D_{2h}^{18}$  and the appearance of orthorhombic twin domains. Although the magnetic structure is well described by a body-centered tetragonal lattice (for the Cu ions) with  $S = \frac{1}{2}$ , we still use the orthorhombic unit cell with four Cu atoms per cell, as shown in Fig. 3 of Ref. 2. The magneto-optical studies on ferromagnetic stripe domains by Kleeman and Schäfer<sup>3</sup> concluded that the [100] axis is the easy axis. The two-dimensional nature of this compound had been investigated by Yamada.<sup>4</sup> From specific heat measurements, the Heisenberg exchange interaction between the spins within the plane perpendicular to the C axis was found to be  $J/k_B = 11.34$  K. The anisotropic coupling constant  $J_A/k_B = 0.089$  K and the interplanar exchange constant  $J_I/k_B = 0.0088$  K, where  $k_B$  is the Boltzmann constant.

It is predicted<sup>5</sup> theoretically that a strictly two-dimensional ferromagnet with Heisenberg or XY symmetry cannot have a critical temperature below which the system is spontaneously magnetized. The existence of a phase transition in this compound at  $T = 6.25$  K is due to the weak interlayer coupling.

$K_2CuF_4$  has been investigated in some detail with unpolarized neutrons. Magnons propagating along the [100] direction, at zero field, have been observed by Funahashi *et al.*,<sup>6</sup> for temperatures both below and well above the

Curie temperature  $[(0.67-2.2)T_C]$ . Two-dimensional magnetic materials are believed to disorder because of the existence of "vortices" (where the local magnetization reverses direction with respect to the mean magnetization) which are bound below  $T_C$  but become unbound above.<sup>7</sup> Moussa and Villain<sup>8</sup> developed a theory for the spin waves in  $K_2CuF_4$  valid for small wavelengths and for temperatures both below and above  $T_C$ . Their theory quantitatively explains the behavior of the spin-wave line shape up to  $1.5T_C$  that was observed in Ref. 6. At higher temperatures their model fails to predict the observed intensity drop, as the integrated magnon intensity is not related to the mean magnetization but is only a result of the two-dimensional short-range order. Preliminary polarization-analysis measurements on  $K_2CuF_4$  were done by Wagner *et al.*<sup>9</sup> In their experiment, unpolarized neutrons were incident on the sample; analysis of the polarization of the scattered neutrons was obtained using a Heusler polarizing crystal. They found that for magnons propagating in the [001] direction and in a field of 10 kG, the integrated magnon intensity for the allowed polarization closely followed the mean magnetization  $m(T)$  up to 6.5 K. This result indicates a connection between the scattered intensity and the mean magnetization. However, the "forbidden" magnon integrated intensity, which was expected to result from unbound vortices, could hardly be distinguished from the background in the temperature and external magnetic field region that they studied. It was argued that forbidden scattering did not occur because of the large amount of long-range order induced by the applied magnetic field.

In this work, we concentrated on the application of relatively low magnetic fields where any induced enhancement of long-range order should be small. From

constant- $Q$  scans the allowed and forbidden magnon excitation frequencies and scattering intensities were extracted from the data at temperatures ranging from just below to well above  $T_C$  ( $0.9T_C$ – $2.8T_C$ ). The relationship between the scattered intensity and the mean magnetization could then be more meaningfully examined. The evolution of both the allowed and forbidden magnon frequencies and linewidths as a function of temperature were also studied.

## II. INSTRUMENTAL DETAILS

Polarized inelastic neutron-scattering measurements were carried out on the triple-axis spectrometer, *H8*, at the High Flux Beam Reactor at Brookhaven National Laboratory. The spectrometer was set up in the *W* configuration to reduce the background as much as possible. A Heusler (111) crystal was used to monochromate and polarize the incident neutrons with an energy  $E_i = 41$  meV ( $\lambda = 1.41$  Å). The scattered neutrons were energy analyzed using the (002) planes of a vertically curved highly oriented pyrolytic graphite (HOPG) crystal. Horizontal collimation angles in the four legs of the spectrometer were  $20', 40', 20', 40'$  (full width at half maximum), respectively. To ensure the desired mutual parallelism of the beam polarization vector  $\mathbf{P}$  and overall sample magnetization vector  $\mathbf{m}$ , and to prevent depolarization of the incident neutron beam by the sample, a horizontal magnetic field  $\mathbf{H}$  was applied along the [100] axis in the scattering plane, while the scattering vector was set to  $(1.2, 0, -1)$  so that we were 40% away from the zone center. This meant that the scattering vector was not exactly parallel to  $\mathbf{P}$  and  $\mathbf{m}$ . The configuration used in our experiment was a compromise situation due to the construction of the electromagnet. In order to achieve both the Bragg peak (for alignment and flipping ratio studies) and the desired scattering angles to cover the required energy transfer range it was impossible to have  $\mathbf{Q}$  exactly parallel to  $\mathbf{H}$ . Consequently, the intensity data obtained for each flipper direction had to be subjected to a “cross-talk” correction between the two polarization states, which to the lowest order is proportional to the square of the cosine of the angle between  $\mathbf{H}$  and  $\mathbf{Q}$ .

A neutron flipper placed between the polarizer and the sample selected the two spin states. Vertical guide fields were placed before and after sample to prevent depolarization of the neutron beam. The sample itself was mounted on a copper post and oriented so that the [010] axis was vertical. It was surrounded by a helium-exchange gas in an Al container attached to the bottom of a variable-temperature cryostat. The temperature of the sample was monitored with a carbon-glass thermometer to within  $\pm 0.1$  K. The temperature stability during the course of a specific scan (typically 3 h) was comparable. The flipping ratios,  $R$ , as a function of field and temperature, were obtained using a fully polarized beam with a Heusler-sample-Heusler set up, by measuring the intensity of the Bragg peak at  $\mathbf{Q} = (2, 0, 0)$ . At each field,  $R$  tended to saturate at a value of  $\sim 19$  near twice  $T_C$ . The depolarization of the neutron beam, in the worst case, caused about a 3% reduction of the polarization,  $P$ ; all the data were corrected for the effects of incomplete polarization.

By measuring the temperature dependence of critical scattering intensity with an applied magnetic field of 3 kG, we obtained the Curie temperature of our sample under these conditions. Critical scattering was measured at  $\mathbf{Q} = (2.5, 0, 0)$ . Data for the two different flipper states were then summed and fitted to a Lorentzian curve. The result gives  $T_C = 6.30 \pm 0.03$  K (a Gaussian fit gives the same peak center but a much worse  $\chi$ ). Our measured  $T_C$  at 3 kG is slightly higher than the generally accepted value of 6.25 K obtained in zero field.

The data were obtained using constant- $Q$  scans at  $\mathbf{Q} = (1.2, 0, -1)$ . The spectrometer was programmed to record the intensities from neutron energy loss of 1–11 meV in steps of 1 meV. The experiment was undertaken with 2- and 3- kG applied fields over the temperature range from 5.6 to 18 K (i.e., from  $0.9T_C$  to  $2.8T_C$ ).

## III. DATA ANALYSIS

The treatment and analysis of the data are described below.

(i) The raw data were fitted to two Gaussians plus a constant background, using a least-square-fitting routine. The first Gaussian simulated the elastic nuclear incoherent scattering, while the second Gaussian described the magnetic excitation. Although there is no theoretical reason for using a Gaussian, our data fit very well to it. (Lorentzian fit gave a much worse  $\chi$ .) The purpose of this step was to obtain the constant background.

(ii) The constant background was subtracted from the raw data.

(iii) Analyzer resolution correction: Measurements were undertaken using constant neutron incident energy. The monochromator scattering angle is fixed during the scan, while varying the analyzer scattering angle to meet the desired neutron energy change. The analyzer therefore detects a different intensity in the scattered beam at each scan point. A correction must be applied to normalize this varying resolution of the analyzer.

(iv) Cross-talk correction between the two polarization states: The magnetic field was applied along the [100] axis, while the scattering vector was set to  $(1.2, 0, -1)$ .  $\mathbf{Q}$  is therefore not parallel to  $\mathbf{m}$ , the offset angle was about  $21^\circ$ . The resulting “geometrical” correction to the experimental data is about 3.7%.

(v) Polarization correction: The incomplete polarization of the incident neutron beam was corrected using the analysis discussed in previous work.<sup>10</sup>

(vi) The reduced data was fitted once more with two Gaussians.

(vii) The Gaussian representing the elastic nuclear incoherent peak was subtracted from the reduced data leaving only the magnetic excitation spectrum.

The results for the different fields and different temperatures are discussed in Secs. IV and V.

Hirakawa and Ubukoshi<sup>11</sup> systematically measured the magnetization of  $\text{K}_2\text{CuF}_4$  as a function of temperature and magnetic field applied both parallel and perpendicular to the  $c$  axis. Their measurements were limited to 11 K in temperature and 0.9 kG in applied magnetic field, while our experiments were taken up to 18 K and in fields of 2

and 3 kG, respectively. Their results show that the magnetization varies linearly with the magnetic field over the temperature region investigated. We assumed this linear behavior remains valid at least up to 3 kG. The values of the magnetization over the range of temperatures and fields used in our experiments were generated from fits to their data and are shown in the insets in Figs. 4 and 8.

#### IV. $H = 3$ kG DATA

Spectra of the allowed and forbidden magnons in a magnetic field of 3 kG were recorded using constant- $Q$  scans [ $Q = (1.2, 0, -1)$ ] at different temperatures in the range from  $0.89T_C$  to  $2.86T_C$ . Each set of data was subjected to the analysis procedure discussed previously. The constant background and nuclear elastic scattering contributions were subtracted; the varying resolution of the analyzer, the cross-talk between two polarization states due to the nonparallel arrangement of the scattering vector and sample magnetization vector, and the incomplete polarization of the incident beam were then corrected. The analyzer reflectivity and the relative Bose-Einstein correction factors are small over the energy and temperature region studied, and therefore were not considered. The 3-kG-reduced data were fitted at each temperature to Gaussian line shapes from which the allowed and forbidden magnon frequencies, linewidths (full width at half maximum) and peak intensities were obtained. The areas under the intensity versus energy curves were used for the integrated intensities.

Figures 1(a) and 1(b) show the comparison of allowed and forbidden magnons at each temperature. At the lowest temperature,  $T = 5.6$  K, a small forbidden component (of about 70 counts) can be discerned around 6.4-meV energy transfer. As temperature is increased, the forbidden excitation become more intense and well defined, while the intensity of the allowed component decreases.

Figures 1(a) and 1(b) clearly show that both the allowed and the forbidden magnons shift to slightly lower frequency with increasing temperature. The width of allowed magnon broadens while that of the forbidden magnon remains approximately the same over the temperature region studied.

In a theory which takes into account the dynamical interactions between pairs of spin waves in a Heisenberg system, the spin-wave dispersion at finite but low temperature  $T$  is given by<sup>12</sup>

$$\begin{aligned} \hbar\omega_q(T) = & 2S[J(0) - J(\mathbf{q})] \\ & - \frac{1}{N} \sum_{\mathbf{k}} \langle n_{\mathbf{k}} \rangle [J(0) - J(\mathbf{q}) + J(\mathbf{k} - \mathbf{q}) - J(\mathbf{k})]. \end{aligned}$$

Although this theory is supposed to be valid for  $T \ll T_C$ , since the magnons due to short-range order that we have here are expected to behave like zero-temperature magnons (with a magnetization equal to the local magnetization), this is not totally unreasonable. The main result of the theory, at small  $q$ , is

$$\hbar\omega_q(T) = D_0(1 - \alpha T^{2.5})q^2.$$

Our  $q$  was 40% away from the zone center. Although the  $Dq^2$  approximation to the dispersion relation is about 13% higher than the exact expression (estimated from Moussa and Villain's<sup>8</sup> dispersion relation calculation at  $T = 12$  K), the fit that includes  $q^4$  term gives only about 5% difference in  $D_0$  and 3% difference in  $\alpha$ . Therefore

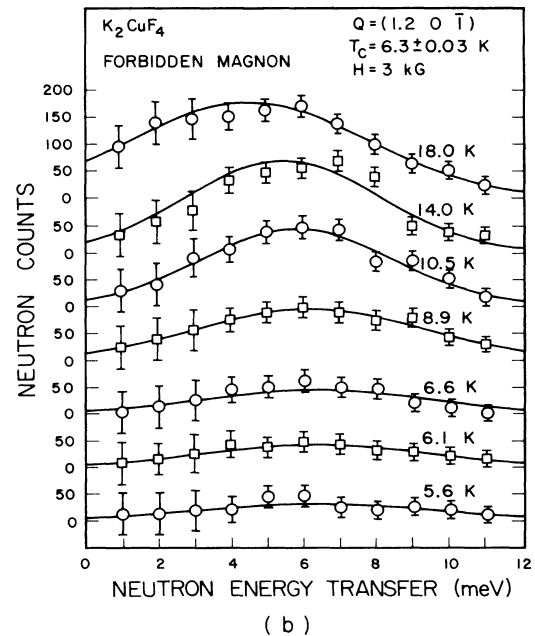
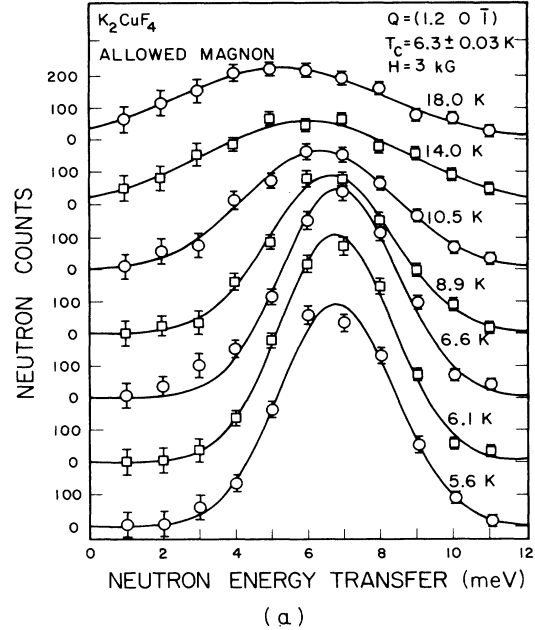


FIG. 1. The (a) allowed and (b) forbidden magnon intensities observed at  $Q = (1.2, 0, -1)$  in a magnetic field of 3 kG applied along the [100] axis, using  $E_i = 41$  meV. The constant background and elastic incoherent peak have been subtracted. The data have also been subjected to analyzer resolution, instrumental depolarization and cross-talk corrections. The solid curves are Gaussian fits to the reduced data.

we assume that  $Dq^2$  expression is still approximately correct in our case. The excitation energies of the allowed and forbidden magnons as a function of  $T^{2.5}$  are plotted in Fig. 2. The values of  $D_0$  and  $\alpha$ , calculated from the least-square fit are  $D_0 = 75 \pm 5 \text{ meV \AA}^2$  and  $\alpha = 0.017 \pm 0.002$  for the allowed magnon results, and  $D_0 = 71 \pm 8 \text{ meV \AA}^2$  and  $\alpha = 0.022 \pm 0.006$  for forbidden magnon where

$$\alpha = \frac{\pi V_0}{S} \frac{R_1^2 J^{(4)}}{J^{(2)}} \left( \frac{k_B}{4\pi D_0} \right)^{5/2} \xi\left(\frac{5}{2}\right),$$

and

$$J^{(n)} = \sum_R J_R (R/R_1)^n,$$

$R_1$  is the nearest-neighbor distance, and  $\xi(n)$  is the Riemann  $\zeta$  function of order  $n$ . The agreement is found to be surprisingly good.

The temperature dependences of energy-integrated intensity for both allowed and forbidden magnons are plotted in Fig. 3 where their sum is shown also. Our results indicate that the forbidden magnon scattering intensity rises steadily over the range of temperature studied, while the allowed integrated intensity falls off. In the absence of an applied magnetic field, the two intensities should join at  $T_C$ ; here we see that the application of a magnetic field effectively displaced this intersection point to higher temperatures. The sum of integrated intensity remains approximately constant, indicating that short-range order persists over a large temperature range. The difference between the allowed and forbidden integrated intensities as a function of the overall magnetization are plotted in Fig. 4. The linear behavior of the difference intensity versus overall magnetization agrees with Ref. 13. Since the theory of Ref. 13, however, is only expected to be valid if we assume that the local magnetization varies

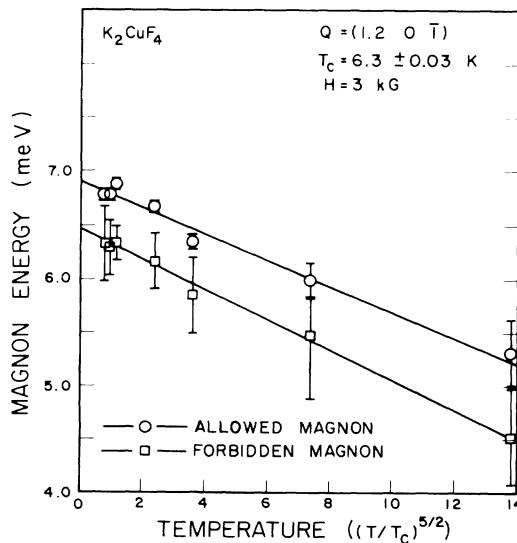


FIG. 2. An energy plot of the allowed and forbidden magnon peaks at  $Q=(1.2, 0, -1)$  as a function of  $(T/T_C)^{5/2}$  at  $H=3 \text{ kG}$ .

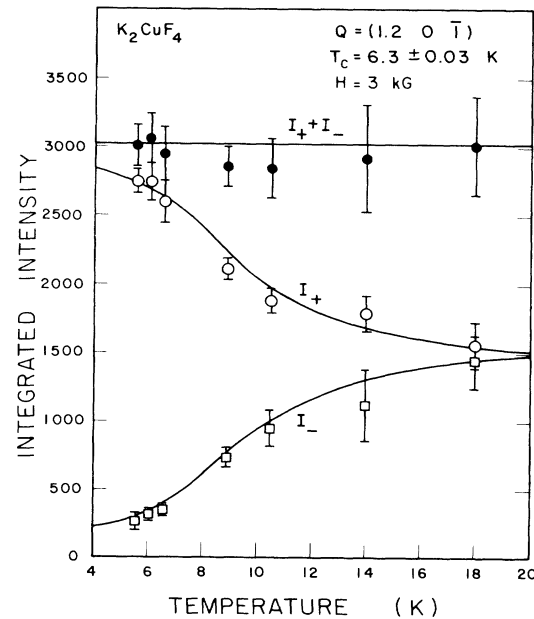


FIG. 3. The allowed ( $I_+$ ), forbidden ( $I_-$ ), and  $I_+ + I_-$  integrated intensities for  $Q=(1.2, 0, -1)$  magnons at  $H=3 \text{ kG}$  as a function of temperature. The intensity data are calculated from the fitted magnon excitation peaks shown in Figs. 1(a) and 1(b). The solid curves are guides to the eye only. The total integrated intensity  $I_+ + I_-$  remains approximately constant over the temperature range (5.6–18 K) investigated.

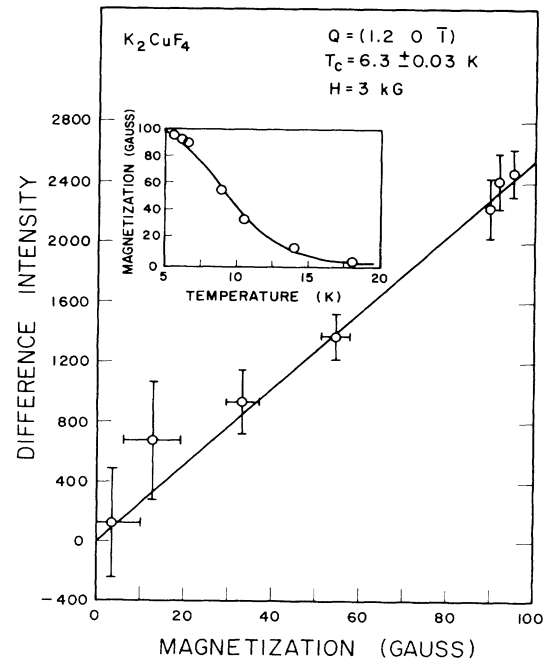


FIG. 4. The difference between the integrated spectral intensities of the allowed and forbidden magnons plotted against the overall magnetization. The values were derived from constant  $Q=(1.2, 0, -1)$  scans with an applied field  $H=3 \text{ kG}$ . The magnetization, shown in the inset, is taken from the data reported by Hirakawa and Ubukoshi (Ref. 11). The linear behavior confirms Sokoloff's prediction (Ref. 13).

very slowly in space over a distance of length comparable to many magnon wavelengths, this is a surprising result.

### V. $H = 2$ kG DATA

Spectra of the (0,2,0,0) allowed and forbidden magnons in a magnetic field of 2 kG were also recorded using constant- $Q$  scans at four different temperatures in the range from  $0.97T_C$  to  $2.54T_C$ . Data were subjected to exactly the same analysis procedure as was undertaken for  $H = 3$  kG data. The allowed and forbidden excitations at each temperature are shown in Figs. 5(a) and 5(b). Comparison of Fig. 1 (3-kG data) with Fig. 5 (2-kG data) shows that the induced long-range order is reduced when a smaller field is applied. A 2-kG field is about the lower limit to maintain a reasonable flipping ratio.

Both the allowed and forbidden magnon frequencies have the same temperature dependence as that of  $H = 3$  kG that we plotted in Fig. 2. Least-square fits gives  $D_0 = 75 \pm 7$  meV  $\text{\AA}^2$  and  $\alpha = 0.016 \pm 0.003$  for the allowed magnon, and  $D_0 = 67 \pm 7$  meV  $\text{\AA}^2$  and  $\alpha = 0.016 \pm 0.003$  for the forbidden magnon. As temperature is increased, the width of forbidden magnon diminishes while the width of its allowed counterpart broadens over the temperature range studied as shown in Fig. 6. The temperature dependence of the energy-integrated intensities is shown in Fig. 7. The difference intensity as a function of the overall magnetization is plotted in Fig. 8. The linear dependence of difference intensity versus the overall magnetization is observed once more.

## VI. DISCUSSION OF THE RESULTS

### A. The "forbidden" intensity

It was argued that,<sup>12</sup> in the vicinity of  $T_C$ , the local magnetization density does not immediately diminish, but rather it is perturbed so that at a temperature sufficiently close to  $T_C$  when the correlation length is many lattice constants long, the neutrons are in an environment with a nearly constant local magnetization. If the local magnetization fluctuation time is long enough for neutrons to travel many lattice constants before the magnetization density appears to change significantly, the magnetic excitations persist. At sufficiently high temperature, the direction of the local magnetization orients over all directions; magnons can therefore be excited by a neutron beam of either polarization.

It is well known that the neutron magnetic scattering cross section is related to the imaginary part of the generalized susceptibility of the target sample. By expressing the forbidden integrated intensity as a fraction of the total scattering intensity, the conversion factors used to correct the data for the individual integrated susceptibilities cancel. Therefore the ratio of the integrated intensities represents the ratio of forbidden integrated susceptibility to the total integrated susceptibility. In an applied field of 3 kG, the forbidden susceptibility has attained only 24% of its final amplitude by  $T_C$ , which indicates a significant induced long-range order by the applied field. A smaller applied field of  $H = 2$  kG reduces the induced enhancement, in this case, the forbidden susceptibility attains

38% of its final amplitude at  $T_C$ . The curves shown in Figs. 3 and 7 qualitatively indicate how the permitted (forbidden) intensity falls (rises) over the range of temperatures studied. Comparing the curves for the two different fields, we see that magnetic field enhances permitted scattering while it diminishes forbidden scattering.

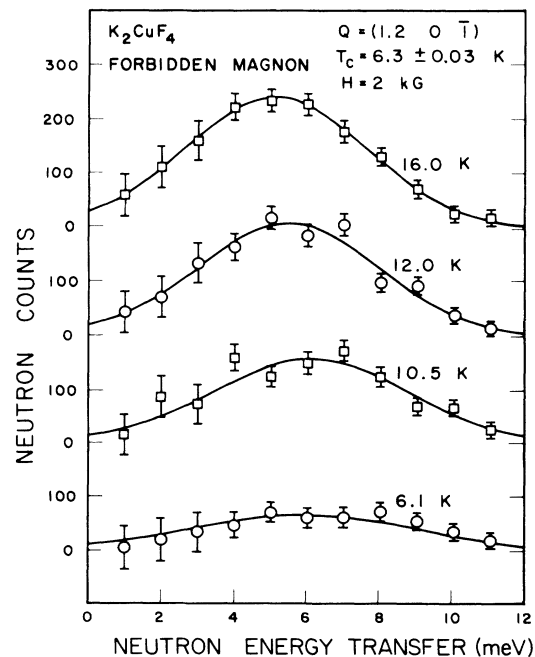
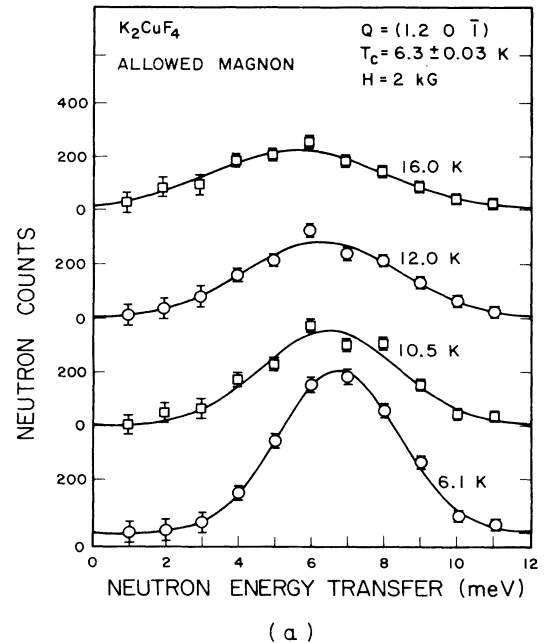


FIG. 5. The (a) allowed and (b) forbidden magnon intensities observed at  $Q = (1.2, 0, -1)$  in a magnetic field of 2 kG applied along the [100] axis, using  $E_i = 41$  meV. The constant background and elastic incoherent peak have been subtracted. The data have also been subjected to analyzer resolution, instrumental depolarization and cross-talk corrections. The solid curves are Gaussian fits to the reduced data.

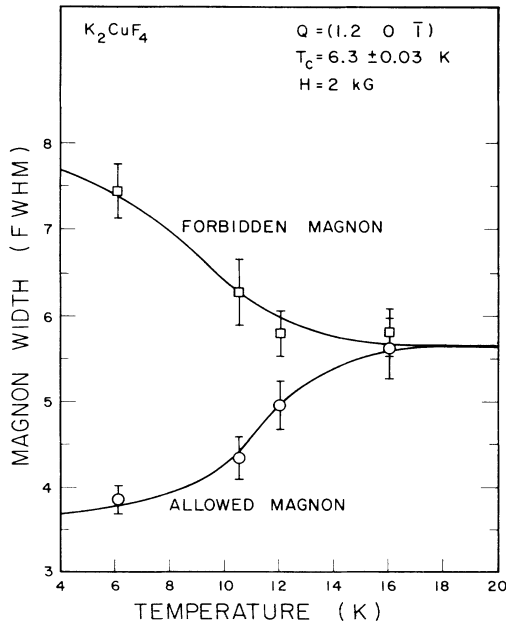


FIG. 6. The observed allowed and forbidden magnon linewidths (full width at half maximum) at  $H=2$  kG. As the temperature is raised from below  $T_C$ , the allowed magnon broadens while the forbidden magnon renormalizes and becomes progressively more well-defined. At  $\sim 2.5T_C$  the allowed and forbidden magnons become indistinguishable. The solid curves are guides to the eye only.

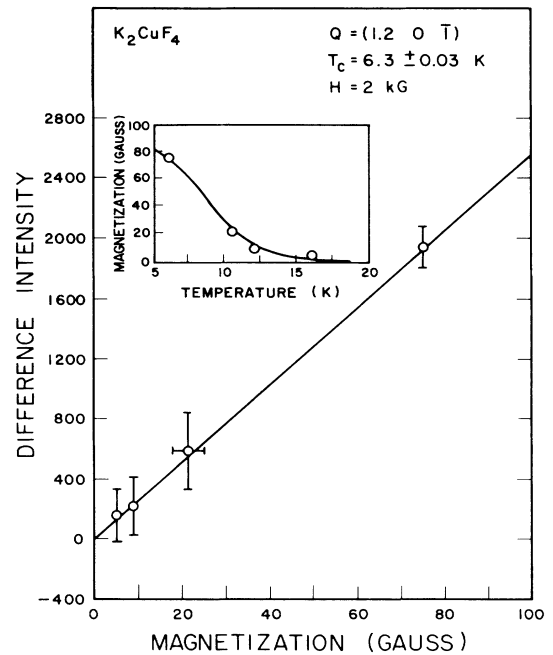


FIG. 8. The difference between the integrated spectral intensities of the allowed and forbidden magnons plotted against the overall magnetization. The values were derived from constant  $\mathbf{Q}=(1.2,0,-1)$  scans with an applied field  $H=2$  kG. The magnetization, shown in the inset, is taken from the data reported by Hirakawa and Ubukoshi (Ref. 11). The linear behavior confirms Sokoloff's prediction (Ref. 13).

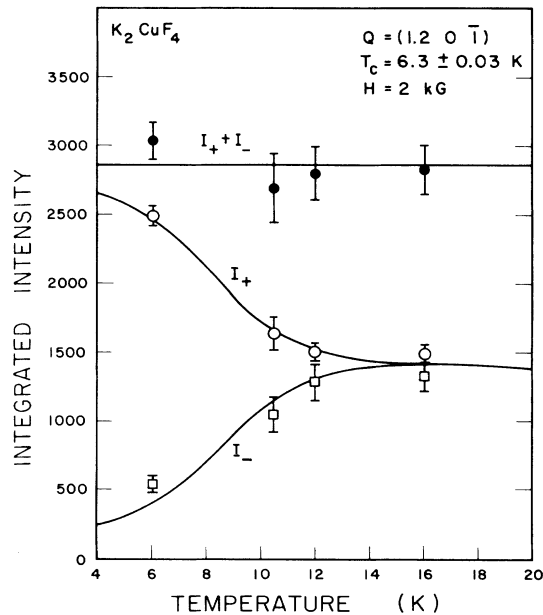


FIG. 7. The allowed ( $I_+$ ), forbidden ( $I_-$ ) and  $I_+ + I_-$  integrated intensities for  $\mathbf{Q}=(1.2,0,-1)$  magnons at  $H=2$  kG as a function of temperature. The intensity data are calculated from the fitted magnon excitation peaks shown in Figs. 5(a) and 5(b). The solid curves are guides to the eye only. The total integrated intensity  $I_+ + I_-$  remains approximately constant over the temperature range (6.1–16 K) investigated.

### B. The difference intensity ( $I^+ - I^-$ )

Based on the "slowly fluctuating spin density picture of ordering of itinerate ferromagnets," Sokoloff<sup>13</sup> has shown that in a special experimental arrangement where  $\mathbf{m} \parallel \mathbf{P} \parallel \mathbf{Q}$ , the polarized neutron scattering cross section is proportional to the imaginary part of

$$\chi = \left[ \frac{1}{3} \pm \frac{1}{2} PL_1 + \frac{1}{6} L_2 \right] \chi^{\mp \pm},$$

where  $P$  is the neutron beam's polarization, and  $L_1$  and  $L_2$  are the first- and second-order Legendre polynomials,

$$L_1(T) = \langle \cos \theta \rangle = m(T)/M(T)$$

and

$$L_2(T) = \left\langle \frac{3}{2} \cos^2 \theta - 1 \right\rangle,$$

related to  $\theta$ , the angle between local magnetization  $\mathbf{M}(T)$  and overall magnetization  $\mathbf{m}(T)$ . The allowed magnon appears in the susceptibility  $\text{Im} \chi^{-+}(\omega)$  while the forbidden magnon appears in  $\text{Im} \chi^{+-}(\omega)$ . Following the expression given by Sokoloff,<sup>13</sup> the difference between the energy-integrated intensities of allowed and forbidden magnons is

$$I_+ - I_- \propto m(T)/M(T).$$

If the microscopic moment at the atomic site is nearly temperature independent, we obtain

$$I_+ - I_- \propto m(T),$$

as we observed in Figs. 4 and 8. We note that from the two fields surveyed, both plots give the same slopes ( $25.8 \pm 1$  for  $H = 3$  kG and  $25.8 \pm 2$  for  $H = 2$  kG). This is in agreement with the linear behavior predicted in most theories of neutron scattering by short-range order, and with the linear dependence on magnetization observed in similar polarized neutron experiments on Ni (Ref. 10) and MnSi (Ref. 14).

### C. Magnon energy shifts

The dynamical interaction between spin waves predicts, within the linear approximation, a  $T^{5/2}$  temperature dependence to the stiffness constant  $D$ .<sup>12</sup> Experimental results on Ni (Ref. 15), Fe (Ref. 15), EuO (Ref. 16) and certain Heusler alloys<sup>17</sup> show that a  $T^{5/2}$  dependence of  $D$  provides a satisfactory account for the behavior of the magnon energies with temperature at temperatures well below  $T_C$ . Our data, Fig. 2, show that both allowed and forbidden magnon energies in  $K_2CuF_4$  also have this temperature dependence at  $Q = (1.2, 0, -1)$  over the temperature region studied.

The local band model proposed by Sokoloff<sup>13</sup> and developed by Korenman and Prange<sup>18</sup> (KP) also predicts a temperature-dependent magnon energy shift. On a microscopic scale the immediate surroundings of an atom are sufficiently ordered that the Stoner theory would apply locally, but the direction of local magnetization remains unconstrained. Following KP's analysis, the magnon energy observed by neutron scattering, close to and above the Curie temperature  $T_C$ , is approximately  $D_0 q_0^2 - (D_0/2)(\nabla \mathbf{M})_{av}^2$ . In terms of local coordinates, the allowed (+) and forbidden (-) magnon energies observed by neutrons are<sup>19</sup>

$$E_{\pm} = D_0 \left[ 1 - \frac{(1 - L_2)^2 \langle v \rangle}{6q_0^2 (\frac{1}{3} \pm \frac{1}{2} L_1 + \frac{1}{6} L_2)} \right] q_0^2,$$

where  $q_0$  is the magnon wave vector at absolute zero temperature, and

$$V(\mathbf{r}) = (\nabla \theta)^2 + (\sin^2 \theta)(\nabla \phi)^2.$$

The quantities  $L_1$ ,  $L_2$ , and  $V$  have a complicated temperature dependence. Lowde *et al.*<sup>10</sup> have obtained an estimate of the temperature-dependent profile of the excitation energy for Ni. At low temperatures, the allowed and forbidden frequencies are well separated with the allowed magnons possessing a higher frequency; the two frequencies then join together at higher temperatures. There is a

region, in the vicinity of  $T_C$  just before the two frequencies join together, where the forbidden frequency increases while the allowed frequency decreases as temperature is raised. This divergence for the forbidden magnon was not observed by us, although we do see well-separated frequencies for the allowed and forbidden magnons in the temperature region studied.

## VII. CONCLUSIONS

We have observed underdamped allowed and forbidden magnon scattering in constant- $Q$  scans for two different applied magnetic fields over the temperature range from  $0.9 T_C$  to  $2.9 T_C$ . To study short-range order, it is necessary to use small fields. The fact that we have followed both allowed and forbidden scattering through  $T_C$  supports the interpretation that the excitations observed above  $T_C$  are magnons. The existence of forbidden scattering at temperature above  $T_C$ , suggests that temperature twists the whole region of spin distribution away from external magnetic field direction. The difference between the allowed and forbidden magnon intensities was found to be directly proportional to the overall magnetization for the two different fields applied. A frequency difference between the allowed magnon and its forbidden counterpart with the allowed magnon being slightly higher was also observed. This result indicates that a special renormalization energy is needed to "twist" the local magnetization direction in the easy plane, as introduced in Sokoloff's,<sup>13</sup> and Korenman and Prange's<sup>18</sup> (SKP) theory for three-dimensional systems. However we do not observe a temperature region, just prior to where the allowed and forbidden magnons become completely indistinguishable, where the forbidden intensity shows a small divergence as suggested by SKP. Whether this is simply because our applied field is too strong, or occurs in a temperature region slightly above the range of our investigation, or the intensity increase is just too small to be observed, or this region does not exist at all in a two-dimensional Heisenberg ferromagnet can only be answered by further, more detailed measurements in this region.

## ACKNOWLEDGMENTS

This work was supported in part by NSF Grant No. DMR 8205480 and NATO Grant No. 1360. The Brookhaven National Laboratory is supported by the Division of Materials Sciences, the United States Department of Energy, under Contract No. DE-AC02-76CH00016.

<sup>1</sup>K. Hirakawa and H. Yoshizawa, J. Phys. Soc. Jpn. **47**, 368 (1979).

<sup>2</sup>M. Hidaka and P. J. Walker, Solid State Commun. **31**, 383 (1979).

<sup>3</sup>W. Kleemann and F. J. Schäfer, J. Magn. Magn. Mater. **21**, 143 (1980).

<sup>4</sup>I. Yamada, J. Phys. Soc. Jpn. **33**, 979 (1972).

<sup>5</sup>N. D. Mermin and H. Wagner, Phys. Rev. Lett. **17**, 1133 (1966).

<sup>6</sup>S. Funahashi, F. Moussa, and M. Steiner, Solid State Commun. **18**, 433 (1976).

<sup>7</sup>J. Kosterlitz and D. Thouless, J. Phys. C **6**, 1181 (1973); J. Kosterlitz, *ibid.* C **7**, 1046 (1974).

<sup>8</sup>F. Moussa and J. Villain, J. Phys. C **9**, 4433 (1976).

- <sup>9</sup>V. Wagner, C. H. Perry, and C. Escribe, *Verh. Dtsch. Phys. Ges.* **15**, 266 (1980).
- <sup>10</sup>R. D. Lowde, R. M. Moon, B. Pagonis, C. H. Perry, J. B. Sokoloff, R. S. Vaughan-Watkins, M. C. K. Wiltshire, and J. Crangle, *J. Phys. F* **13**, 249 (1983).
- <sup>11</sup>K. Hirakawa and K. Ubukoshi, *J. Phys. Soc. Jpn.* **50**, 1909 (1981).
- <sup>12</sup>S. W. Lovesey, *Theory of Neutron Scattering from Condensed Matter*, (Clarendon, Oxford, 1984).
- <sup>13</sup>J. B. Sokoloff, *J. Phys. F* **5**, 1946 (1975).
- <sup>14</sup>J. B. Sokoloff, W. H. Li, B. Pagonis, C. H. Perry, C. F. Majkrzak, G. Shirane, and Y. Ishikawa, *Solid State Commun.* **52**, 693 (1984).
- <sup>15</sup>M. W. Stringfellow, *J. Phys. C* **1**, 950 (1968).
- <sup>16</sup>C. J. Glinka, V. J. Minkiewicz, and L. Passell, *Magnetism and Magnetic Materials (Boston, 1973)*, Proceedings of the 19th Annual Conference on Magnetism and Magnetic Materials. AIP Conf. Proc. No. 18, edited by C. D. Graham and J. J. Rhyne (AIP, New York, 1974).
- <sup>17</sup>Y. Ishikawa and Y. Noda, *Magnetism and Magnetic Materials (San Francisco, 1974)*, Proceedings of the 20th Annual Conference on Magnetism and Magnetic Materials. AIP Conf. Proc. No. 24, edited by C. D. Graham, G. H. Lander, and J. J. Rhyne (AIP, New York, 1975).
- <sup>18</sup>V. Korenman, J. L. Murray, and R. E. Prange, *Phys. Rev. B* **16**, 4032 (1977); **16**, 4048 (1977); **16**, 4058 (1977).
- <sup>19</sup>V. Korenman and R. E. Prange, *J. Magn. Magn. Mater.* **15-18**, 355 (1980).